MASS TRANSFER IN OSCILLATING FLOWS

Efficient Drying via Pulse Combustors

FINAL REPORT

January 1988 - September 1991

Gas Research Institute
8600 West Bryn Mawr Avenue
Chicago, Illinois 60631

MASS TRANSFER IN OSCILLATING FLOWS - EFFICIENT DRYING VIA PULSE COMBUSTORS

FINAL REPORT

January 1988 - September 1991

Prepared by

V. S. ARPACI and R. GEMMEN

University of Michigan

For

GAS RESEARCH INSTITUTE

GRI CONTRACT NO. 5088-260-1686

GRI Project Manager

Ferol Fish

Physical Sciences Department

APRIL 1992

GRI DISCLAIMER

LEGAL Notice. This report was prepared by the University of Michigan as an account of work sponsored by the Gas Research Institute (GRI). Neither GRI, members of GRI, nor any person acting on behalf of either:

a. Makes any warranty or representation, express or implied, with respect to the accuracy, completeness, or usefulness of the information contained in this report, or that the use of any apparatus, method, or process disclosed in this report may not infringe privately owned rights; or

b. Assumes any liability with respect to the use of, or for damages resulting from the use of, any information, apparatus, method, or process disclosed in this report.

272-101

REPORT DOCUMENTATION PAGE	1. REPORT NO.	2.	3. Recipient's Accession No.

4. Title and Subtitle

Mass Transfer in Oscillating Flows - Efficient Drying via Pulse Combustors

5. Report Date
January 1992

6.

7. Author(s)
V. S. Arpaci and R. Gemmen

8. Performing Organization Rept. No.

9. Performing Organization Name and Address
Mechanical Engineering Department
University of Michigan
Ann Arbor, MI 48109-2125

10. Project/Task/Work Unit No.

11. Contract(C) or Grant(G) No.
(C) 5088-260-1686
(G)

12. Sponsoring Organization Name and Address
Gas Research Institute
8600 West Bryn Mawr Avenue
Chicago, IL 60631

13. Type of Report & Period Covered
Final Report
Jan 1988 - Dec 1991

14.

15. Supplementary Notes

Experimental part of the study was carried out at the Sandia National Laboratories. Analytical part was carried out at the University of Michigan.

16. Abstract (Limit: 200 words)

Pulse combustors are known to have high rates of heat and mass transfer in the tailpipe because of velocity oscillations created by the acoustic resonance of the combustor. The results so far reported in the literature are inconclusive.

A study of the mass transfer rates in a pulse combustor tailpipe has been conducted. The significant parameters including mean flow rate, frequency and amplitude of pulsation were varied nearly independently and their effects on the mass transfer were investigated. The mass transfer in the tailpipe is found to be enhanced by the oscillations up to a factor of 2 over steady turbulent flow. A correlation for mass transfer in pulsating turbulent flow is developed using a novel approach based on the appropriate microscales of turbulence and guided by the physical insight gained from experiments. The final form of the correlation will be available upon the completion of a doctoral thesis which is being written.

17. Document Analysis a. Descriptors

Pulse combustor
Mass transfer
Turbulent flow
Mass transfer correlation

b. Identifiers/Open-Ended Terms

c. COSATI Field/Group

18. Availability Statement:	19. Security Class (This Report) Unclassified	21. No. of Pages 80
	20. Security Class (This Page)	22. Price

RESEARCH SUMMARY

Title	Mass Transfer in Oscillating Flows - Efficient Drying via Pulse Combustors
Contractor	University of Michigan GRI Contract No. 5088-260-1686
Principal Investigator	V. S. Arpaci
Co-Principal Investigator	R. Gemmen
Reporting Period	January 1988 - September 1991
Objectives	There are three objectives of this study. The first is to determine if there is a significant mass transfer enhancement in pulse combustor tailpipes, and to determine how this enhancement is affected by the pulsating flow parameters. The second is to gain an understanding of oscillating turbulent flows and mass transfer in these flows. The third is to develop a mass transfer correlation which can be used to predict drying in pulse combustors.

Technical Respective

The need for efficient combustion systems has revitalized research in pulse combustion. One advantage of pulse combustor heating systems is a high rate of heat and mass transfer in the tailpipe. These high rates result from large velocity oscillations occuring in the tailpipe as a result of the acoustic resonance on the pulse combustor. Past experimental research on the effect of flow oscillations on the mass transfer rate found rates higher than those found in steady turbulent flow at the same mean Reynolds number. However, past research has failed to provide an adequate mass transfer correlation for this type of flows.

Results

The mass transfer rates in the tailpipe were found to be enhanced up to a factor of 2 times the expected value for steady turbulent flow. Although the heat transfer increases with both oscillation frequency and velocity oscillation amplitude, mass transfer is found to increase only with amplitude but not frequency. This contradiction is related to the difference between the characteristic lengths involved with heat and mass transfer. The length for heat transfer is that of tailpipe and the length for mass transfer is the length of flat plate or the diameter of the cylinder which are order of magnitude smaller than the tailpipe.

The effects of pressure amplitude, frequency and mean mass flow on mass transfer were obtained experimentally. An analytical model is proposed for mass transfer correlation in oscillating flows.

$$\frac{m'}{\rho D Re^{3/4} Sc^{1/3}} = \frac{C B}{(1 + B)^{3/4}} \left(1 + C_1 \frac{U_o}{\bar{U}}\right)^{3/4} \left(1 + C_2 \frac{\omega \ell}{\bar{U}}\right)^{3/4}$$

The constants of this model are being evaluated by the experimental data and will be reported later.

Technical Approach

Experimental work was carried out at Sandia National Laboratories. A Helmholtz-type pulse combustor with cross-sections for both the combustion chamber (75mm x 75 mm) and tailpipe (30mm x 30mm) convenient for optical diagnostics was used. The tailpipe is double-walled for controlled external cooling. The burner was operated premixed (air and either natural gas or methane) with on-axis injection. The set of controlling parameters for operating conditions are mass flow rates of fuel, air and nitrogen diluent, the tailpipe length and the position of injector stagnation plate.

Project Implications

The mass transfer in pulse combustor tailpipes has been poorly understood. This contract has provided experimental data and a theoretical underpinning for understanding and predicting mass transfer and hence the drying action in pulse combustors.

GRI Project Manager
Ferol Fish
Principal Scientist, Engineering Sciences
Physical Sciences Department

This final report consists of four chapters, the first three being individual conference papers. Since each chapter is written to stand alone, each has its own introduction, literature survey and reference list. The last chapter is a draft of a manuscript under preparation.

CHAPTER 1

PULSE COMBUSTION: NUMERICAL ANALYSIS OF DROPLET MASS TRANSFER ENHANCEMENT

PULSE COMBUSTION: NUMERICAL ANALYSIS OF DROPLET MASS TRANSFER ENHANCEMENT*

R. S. Gemmen
University of Michigan
Ann Arbor, Michigan

J. O. Keller
Combustion Research Facility
Sandia National Laboratories
Livermore, California

V. S. Arpaci
University of Michigan
Ann Arbor, Michigan

ABSTRACT

The effect of a resonant acoustic field on the rate of evaporation of a liquid droplet is investigated using a numerical technique. The resonating acoustic field under consideration is one produced by a pulse combustor. Calculations based on a quasi-steady analysis are performed for the droplet position, velocity, and size. Calculations are also performed to determine the effect of the unsteady pulsating free stream motion on the dynamics of a droplet. The model takes into account the transport of mass, momentum and energy using contemporary correlations for the Sherwood number, drag coefficient and Nusselt number. These correlations have been modified to include effects of blowing at the droplet surface. Various conditions of pulsating flows are investigated and comparisons are made with those of steady flow. The numerical results indicate that evaporation rates are increased by at least 160% over steady flow at the same mean Reynolds number.

NOMENCLATURE

A	=	Cross sectional area.
a	=	Acceleration.
B_H	=	Heat transfer number--defined in the appendix.
B_M	=	Mass transfer number--defined in the appendix.
c	=	Speed of sound.
c_p	=	Evaporating species' gas phase specific heat.
C_D	=	Drag coefficient--defined in the appendix.
D'	=	Form drag coefficient.
D	=	Diffusion coefficient.
d	=	Droplet diameter.
Eo_a	=	Eötvos number for droplet breakup.
F	=	Force.
F_s	=	Force determined from a steady drag coefficient.
h	=	Heat transfer coefficient--defined in the appendix.
h_m	=	Mass transfer coefficient--defined in the appendix.
k	=	Thermal conductivity coefficient.
Le	=	Lewis number--defined in the appendix.
L_e	=	Tailpipe length.
L_s	=	Latent heat of vaporization.
M	=	Mach number.
m	=	Particle mass.
m''	=	Mass flux.
Nu	=	Nusselt number--defined in the appendix.
N_{St}	=	Stokes number.
Pr	=	Prandtl number--defined in the appendix.
P	=	Pressure amplitude.
p'	=	Oscillating component to the pressure.
q''	=	Heat flux.
Q'	=	Oscillating component to energy input.
R	=	Droplet radius.
Re	=	Reynolds number--defined in the appendix.
Sc	=	Schmidt number--defined in the appendix.
Sh	=	Sherwood number--defined in the appendix.
t	=	Time.
Te_e	=	Gas exit temperature to tailpipe.
Te_i	=	Gas inlet temperature to tailpipe.
Te	=	Local temperature of the droplet surroundings.
Ts	=	Temperature at the droplet surface.
Ts'	=	Oscillating component to surface temperature.
Um	=	Steady component to tailpipe gas.
Uo	=	Oscillating component to tailpipe gas.
Uo_d	=	Oscillating amplitude of droplet.
Uo_e	=	Oscillating amplitude of fluid.
ΔV	=	Droplet slip velocity.
V,v	=	Velocity.
V_∞	=	Free steam velocity.
We	=	Weber number for droplet breakup.
x	=	Particle position.
Ys	=	Evaporating species droplet surface mass fraction.
Ye	=	Evaporating species free stream mass fraction.
α	=	Thermal diffusion coefficient.
β	=	D^2 Law evaporation coefficient.
δ	=	Penetration depth.
ε	=	Emissivity.
μ	=	Dynamic viscosity.
ν	=	Momentum diffusion coefficient.
ρ	=	Density.
σ	=	Surface Tension or Stefan-Boltzmann constant.
ω	=	Pulse combustion frequency.

Subscripts:

c	=	Convective term.
e	=	External gas parameter.
B	=	Basset term.
f	=	Fluid/tailpipe gas.
l	=	Liquid parameter.
o	=	Initial condition.
p	=	Particle/droplet or Pressure term.
r	=	Radiation/reduced (film) properties.
s	=	Droplet surface parameter.
w	=	Tailpipe wall term.

* This work was performed at the Combustion Research Facility, Sandia National Laboratories and was supported by the U.S. Department of Energy, Energy Conversion and Utilization Technologies Program, and the Gas Research Institute.

INTRODUCTION

Pulse combustion devices are known for the strong oscillating flows in their resonance tubes. In the tailpipe of a Helmholtz resonator, for example, oscillation amplitudes can reach 100 m/s and pulsation frequencies can range between 50 and 170 Hz.

While knowledge of the processes occurring in both the tailpipe and combustion chamber have steadily increased over recent years (Keller et al. (1989), Dec and Keller (1988, 1989), Dec (1988), Barr et al. (1990, 1989)), most experimental and theoretical studies to date have focused on the combustion processes and heat transfer enhancement aspects. Another important area that has yet to be adequately investigated is the mass transfer enhancement in these devices. In the United States alone, the energy budget for mass transfer related processes is about one Quad/year, Anon (1977), and in the United Kingdom approximately 7% of the total energy budget is devoted to drying processes, Mujundar (1980). Given the large enhancement found in heat transfer for pulse combustors, it is reasonable to expect equally strong enhancement for mass transfer, thus significant energy savings could be achieved by adapting these devices to mass transfer related industrial processes.

This paper presents the results from a numerical investigation on the evaporation rates of freely moving droplets placed inside the tailpipe of a pulse combustor. Many detailed numerical models have been developed that describe the processes occurring in and around an evaporating droplet (Law and Sirignano (1977), Prakash and Sirignano (1980), Renksizbulut and Yuen (1983a), Dwyer and Sanders (1984), Sanders and Dwyer (1986), Tong and Sirignano (1987)). These models have been mostly applied to steady convecting environments. Tong and Sirignano, however, used their model to evaluate the effect of an oscillating flow field on droplet evaporation rates obtaining estimates for combustion instability. Their model assumes a quasi-steady gas phase neglecting the effect of the pressure field on the viscous boundary layer. One achievement from the work of Renksizbulut and Yuen was providing a correlation for the energy transport to a droplet that takes into account evaporative blowing. By using correlations for the transports of mass and energy, the current problem becomes less computationally intensive than those above. The model developed in this study assumes quasi-steady correlations for the transport of mass, momentum and energy. The validity of a quasi-steady analysis is discussed as well as the validity of several other simplifying assumptions. In particular, the effect of unsteady gas/droplet motion on the droplet drag force is neglected. The importance of this unsteady motion to the droplet dynamics is investigated in some detail at the end of the paper once the motion of a droplet has been determined. Other secondary effects on the evaporation rate such as that due to liquid heating/cooling in an unsteady flow are also examined.

DROPLET EVAPORATION MODEL

In the model, a droplet is injected into the entrance of the tailpipe, and calculations for the droplet velocity, position and size are performed for different operating conditions. While the use of empirical correlations for the Nusselt and Sherwood numbers implicitly assumes that the droplet shape is the same as that for steady flow, for all droplet diameter, d, calculations it is assumed that the droplet is spherical. Variable properties are considered through film relations that are specified by the correlations used for the transport quantities. Operating conditions are prescribed based on known values of typical velocity and temperature profiles through the tailpipe. The analysis considers several different oscillating flow conditions and compares these results to those of steady flow at the same mean tailpipe Reynolds number.

Droplet Size Considerations--Droplet Breakup In Accelerated Flows

The initial droplet size for this study was determined by expected droplet sizes for this flow field. In accelerated flows, such as those in a pulse combustor, the acceleration between the droplet and the gas may cause the droplet to break apart. The breakup of a droplet depends on the Eötvos number that describes the surface instability for a liquid droplet under acceleration, Clift et al (1978), and is given by:

$$Eo_a = a\Delta\rho d^2/\sigma \qquad (1)$$

Here, a is the relative acceleration between the two phases, d is the droplet diameter, σ is the surface tension, and $\Delta\rho$ is the density difference between the liquid and gas. The critical Eötvos number for droplet breakup is 16. For $Eo_a>16$, which for the typical pulse combustion operating conditions analyzed in this paper corresponds to diameter droplets greater than 100 μm, the droplet breaks apart. Therefore, the present study will focus on the evaporation rates of droplets with diameters 100 μm and less.

The Use of Quasi-Steady Correlations for the Gas Phase Transport

To model the gas phase transports, correlations for Sherwood number, Sh, Nusselt number, Nu, and drag coefficient, C_D, for steady flows are employed. The quasi-steady gas transport assumption has been found to work reasonably well for droplets with zero slip velocity, Hubbard et al. (1975) and pressures away from the critical point. This assumption need to be investigated more thoroughly, however, for the droplet sizes and velocities considered here which are on the order of 100 μm and 100 m/s respectively. For a quasi-steady gas phase analysis to be valid, the boundary layer motion over the transport surface must be similar to that of steady flow at any given instant. In an acoustic flow, however, the pressure gradient and oscillating gas motion causes boundary layers to phase lead the free stream, Dec et al. (1988), making the quasi-steady analysis fundamentally incorrect. The experimental data on tailpipe wall heat transfer enhancement presented by Dec and Keller (1989) show that quasi-steady theories correctly predict the trends in Nusselt number with pulsation amplitude and mean Reynolds number. Quasi-steady theories, however, will under predict the magnitude of the Nusselt number, sometimes by as much as a factor of 1.5, moreover they inherently contain no frequency effects. While the present study is concerned with heat (and mass) transfer from a liquid surface instead of a solid wall, these results would indicate that the present quasi-steady analysis should provide a conservative estimate for the mass transport enhancement. It should be emphasized, however, that since the flow over a liquid sphere is quite distinct from that over a flat plate, the results from Dec and Keller may not apply. Rigorous testing of these assumptions will have to await experimental verification.

Aside from the effects produced by the pressure, other kinematic effects produced by the gas phase motion can also prevent the use of a quasi-steady analysis. Quasi-steady criteria for convecting flows are: 1.) that the characteristic time for a gas element to flow over a droplet, $d/\Delta V$, must be much less than the characteristic time for the droplet to change its diameter, $d/(dd/dt)$, and 2.) the time for velocity change, $1/\omega$, should be much longer than the characteristic time for diffusion to occur through the boundary layer, e.g. $1/\omega > d/(D\mathrm{Re}^{1/2})$. For typical pulse combustor operating conditions, these requirements are satisfied over most of the droplet life (about 90%). Hence, as far as the gas phase kinematics is concerned (neglecting pressure effects), the process of evaporation can be adequately described by quasi-steady relations.

Liquid Phase Transport Considerations

The liquid phase behavior is neglected by assuming that the liquid droplet is injected at its evaporation (saturation) temperature and therefore undergoes no heating or cooling, and that no species diffusion occurs within the liquid. For the liquid considered in this study (pure water) these assumptions are valid, since the effects of thermal/species transients are weak due to its low boiling temperature, high heat of vaporization, and the fact that species diffusion is non-existent. Detailed numerical solutions have shown, however, that liquid transients can be important (adding more than 10% to droplet lifetime) under certain combinations of evaporating environments and droplet thermodynamic properties, Prakash and Sirignano (1980), Dwyer and Sanders (1984), Tong and Sirignano (1987). The

significance of the liquid heating can be estimated from $c_{pl}\Delta T/h_{fg}$ Where c_{pl} is the heat capacity of the liquid, and ΔT is the liquid temperature change. For water, this parameter is about 6%, whereas for hydrocarbons its value is about 30%. The numerical model can be extended to account for liquid transient effects by including models for the liquid side temperature and/or species fields (Law and Sirignano (1977), Talley and Yao (1984)). For other liquids, this may become necessary.

Droplet Dynamics Model--Quasi-Steady C_D Term

There are two primary flow regimes associated with the motion of a droplet over the range of Reynolds numbers ($0 < Re < 200$) typically found in a pulse combustor. At low Reynolds numbers ($Re \approx 1$) and a non-accelerating flow, the flow over a sphere is one of Stokes flow and the drag forces for a solid sphere is given by Stokes law. For a liquid droplet, the drag is reduced somewhat due to the motion of the liquid which assumes a Hills vortex, Prakash and Sirignano (1980). Blowing at the surface due to evaporation will reduce the viscous transport of momentum thereby reducing the drag. As the Reynolds number increases, the flow over the rearward face of the droplet separates causing form drag. Blowing at the surface can cause this separation of the boundary layer to occur earlier, thereby increasing the form drag.

For strong unsteady droplet and fluid motion, the total force on a droplet is found to be significantly different than that for steady flow at the same Reynolds number. The additional forces result from the pressure gradient driving the flow and the unsteady gas motion:

$$F_{total} = F_S + F_p + F_a + F_B \tag{2}$$

where F_{total} is the total droplet force, F_S is a force determined from a steady drag coefficient, F_p is the pressure gradient force (a form drag component not included in the F_S term due to its definition), F_a is the force produced by accelerating fluid past the droplet, and F_B is the force due to the unsteady motion. For small Re values, an equation for the particle motion containing these parameters is, Hinze (1959) and Briffa (1981):

$$\overbrace{\frac{\pi d^3}{6}\rho_p\frac{dV_p}{dt}}^{F_S} = \overbrace{3d\pi\mu(V_e - V_p)}^{F_p} + \overbrace{\frac{\pi d^3}{6}\rho_e\frac{dV_e}{dt} + \frac{1}{2}\frac{\pi d^3}{6}\rho_e\left(\frac{dV_e}{dt} - \frac{dV_p}{dt}\right)}^{F_a} + \overbrace{\frac{3d^2}{2}\sqrt{\pi\rho_e\mu}\int_0^t \frac{\left(\frac{dV_e}{dt} - \frac{dV_p}{dt}\right)}{\sqrt{t - \tau}}d\tau}^{F_B} \tag{3}$$

where μ is the free stream viscosity, t is time, V_p is the droplet/particle velocity and V_e is the instantaneous free stream velocity. This equation is based on assumptions that restrict its use to low particle Reynolds numbers ($Re \approx 1$). Briffa, however, in the experimental and theoretical analysis of decelerating spray droplets, applied a modified form of Eq. (3) with reasonably good success even with Reynolds numbers approaching 150. This modification adds the following term to the right hand side of Eq. (3):

$$-D'\rho_e\frac{\pi d^2}{4}(V_e - V_p)^2 \tag{4}$$

where D' is a form drag coefficient. This term models a flow regime in which the viscous term is negligible. These two terms (Eq. (4) and the viscous drag term of Eq. (3)) can be reduced to a single term by using a drag coefficient which covers both the low and high regimes of drag on a sphere. This is done in the present model by employing a modified standard drag coefficient as described below.

For a droplet inside a pulse combustor tailpipe, the pressure gradient term, F_p, is negligible as shown in the following relations. The force on a droplet due to free stream pressure gradients is:

$$F_p = (dP/dx)(\pi d^3/6) \tag{5}$$

where F_p is the estimated force on a droplet due to the pressure field, P is the local pressure, x is a spatial location, and d is the droplet diameter. The force determined from a steady drag coefficient is:

$$F_S = 1/2\rho_e C_D(\Delta V)^2 d^2\pi/4 \tag{6}$$

Since the oscillation pressure P is proportional to velocity oscillation amplitude as $P = U_{oe}\rho_e c$, one can write for the ratio of F_p to F_S:

$$F_p/F_S = d/(ML_eC_D) \tag{7}$$

where U_{oe} is the velocity oscillation amplitude, M is a ratio of velocities given by U_{oe}/c, L_e is the tailpipe length, and c is the sound speed of the gas. Estimating these terms to an order of magnitude gives: $d=O(10^{-4})$, $M=O(10^{-1})$, $L_e=O(1)$, $C_D=O(1)$. Therefore, $F_p/F_S = O(10^{-3})$, showing that for droplets of diameter 100μm, the pressure force can be neglected in Eq. (2) relative to the quasi-steady force.

The third and fourth terms in Eq. (3) are also neglected. The third term is negligible, since $(dV_e/dt - dV_p/dt) < dV_e/dt$ which was already shown to be negligible in the second term of Eq. (3). The fourth term in Eq. (2) is more difficult to analyze, since little is known about the effect of strong accelerating flows on the droplet drag. The validity of neglecting this term will be considered in greater detail in the Discussion section.

The only remaining force to be considered in the model for the droplet motion is the quasi-steady drag force, F_S. A drag coefficient for a sphere (modified to include the effects of droplet surface motion as well as blowing due to evaporation from the surface) will be used to model the quasi-steady force, Renksizbulut and Yuen (1983a, 1983b):

$$C_D(1+B_M)^{0.2} = \frac{24}{Re}\left[1 + 0.2Re^{0.63}\right] \qquad 10 < Re < 260 \tag{8}$$

where Re is the Reynolds number of the droplet and B_M is a mass transfer number to be described below. The evaluation of properties (except for ρ_f in Re for the drag coefficient which is taken as the free stream value) is given by a film reference state as:

$$\begin{aligned} Y_r &= Y_S + (Y_e - Y_S)/r \\ T_r &= T_S + (T_e - T_S)/r \\ r &= 2 \text{ for the Renksizbulut-Yuen film model.} \end{aligned} \tag{9}$$

where Y is the mass fraction and T is the temperature.

With the force on the droplet known, the motion of the droplet is determined based on its initial condition (position and velocity) and a fourth order Runge Kutte integration of:

$$\frac{d^2x}{dt^2} = F_S/m \tag{10}$$

where x is the particle position and m is the particle mass.

Droplet Evaporation Model--Sh and Nu Terms

To determine the droplet evaporation rate, the numerical model uses a mass transfer correlation taking into account the surface motion and surface blowing. For the mass transfer coefficient, a correlation for the Sherwood number, Sh, given by Renksizbulut (1989) is:

$$Sh(1+B_M)^{0.7} = 2. + 0.87Re^{1/2}Sc^{1/3} \qquad B_M = \frac{Ys-Ye}{1-Ys} \qquad (11)$$

$$25 < Re < 2000$$

where Re is the Reynolds number, Sc is the Schmidt number and B_M is a potential for mass transfer. The evaluation of all properties is at the film condition described in Eq. (9).

The energy for evaporation is assumed to be due to both radiation and convection to the droplet surface, $q''_s = q''_r + q''_c$ (recall that liquid heating is assumed to be zero and no chemical reactions are considered). For convection, q''_c, the model uses a correlation for the Nusselt number, Nu, given by Renksizbulut and Yuen (1983a, 1983b):

$$Nu(1+B_H)^{0.7} = 2. + 0.57Re^{1/2}Pr^{1/3} \qquad B_H = \frac{c_p(Te-Ts)}{L_s - \left[q''_r/m''\right]_s} \qquad (12)$$

$$25 < Re < 2000$$

where Pr is the Prandtl number, and B_H is a potential for heat transfer, and $[q''_r/m'']_s$ is the ratio of radiation heat flux to mass flux at the droplet surface. This correlation for the energy transfer was used with reasonable success by Tally and Yao (1984) in the prediction of the accelerated droplet motion in a steady flow.

For radiation from the surroundings, the model uses:

$$q''_r = \varepsilon\sigma(T_w^4 - Ts^4) \qquad (13)$$

where ε is the emissivity of the droplet, σ is the Stefan-Boltzmann constant and T_w, the tailpipe wall temperature, is specified based on tailpipe wall data. For the droplet emissivity, the value of 0.96 for water was used, Incropera and DeWitt (1981).

In general, mass transport from a droplet involves the coupling between mass, momentum and energy. The coupling results directly from the processes occurring at the liquid surface (balance of mass/energy), as well as due to secondary effects such as the variation of fluid properties through the boundary layer which often times becomes very significant. The coupling at the droplet surface boundary is given by:

$$v_s = m''_s/\rho_e \qquad (14)$$

$$q''_s = L_s m''_s \qquad (15)$$

$$F(Ps, Ts, Ys_i) \qquad (16)$$

where v_s is the surface normal velocity component and F() is an equation describing the relation between the liquid surface properties, where Ps is the total pressure at the surface, Ts is the surface temperature, and Ys_i is the mass fraction of species in the environment.

Following others, the assumption of surface equilibrium is made, and an equation of state is used to provide the relationship between the surface temperature and surface concentration. In the model, these surface potentials are related via a curve-fit to the Clausius-Clapeyron equation, see Appendix.

Once the surface conditions and transfer coefficients have been iteratively solved, the evaporation rate is given by:

$$m''_s = h_m B_M \qquad (17)$$

$$dd/dt = 2m''_s\rho_e/\rho_l \qquad (18)$$

where h_m is the mass transfer coefficient and ρ_l is the liquid density. The numerical integration of Eq. (19) provides the necessary information on the evolution of the droplet size.

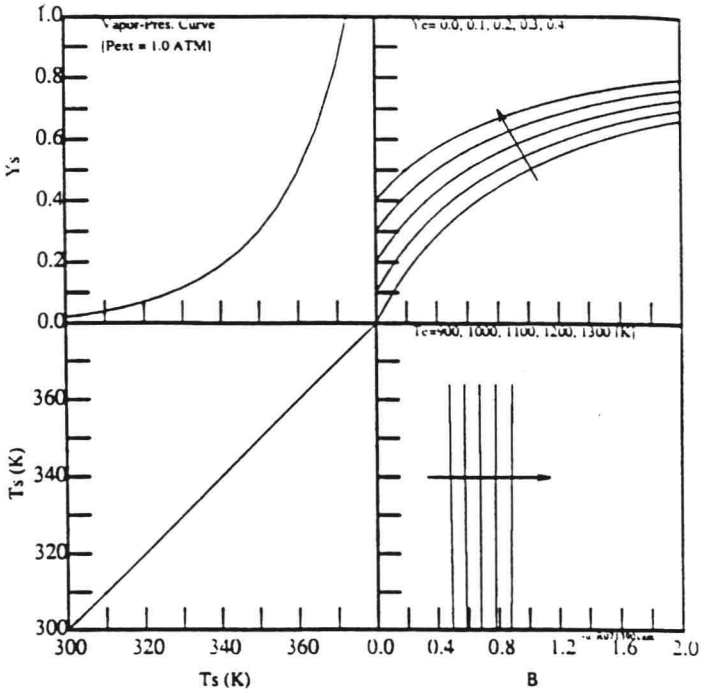

Figure 1. Nomograph for Quiescent Evaporation of Liquid Water (Le = 1). At high external gas temperatures, Te > 350, the evaporation is heat transfer controlled. $B=B_M=B_H$.

Evaluating Surface Conditions--Quiescent Environments

A good understanding of the coupling between mass and energy and the relative effects of these transports on surface conditions can be achieved by examining a droplet in a quiescent environment. For this case, the coupling can be expressed in graphical form as in Figure 1 which is for liquid water at one atmosphere with a gas Lewis number, Le (= α/D = Sc/Pr) = 1. Figure 1 shows how the external potentials for heat and mass transfer affect the surface conditions of the water droplet. In this case, the driving potentials for heat and mass transport, B_H and B_M, respectively, are the same:

$$B_H = B_M = B \qquad (19)$$

In the use of Figure 1, the selection of appropriate curves for Ye and Te is made based on the free stream conditions and an iterative process is performed until the correct surface condition (Ys and Ts) has been determined. This process is started by assuming a value for the droplet surface temperature (a point selected on the lower left plot). A line is
drawn to the right to intersect the selected B curve, then up to the selected Ye curve, then left to the vapor pressure curve and back down to the starting line on the lower left plot. This process continues until the surface temperature converges.

Figure 1 shows how the external potential for heat transfer, Te, dominates the selection of the driving potential B under high evaporation temperatures (the lines in the lower right plot are nearly vertical). The driving potential for heat transfer dominates in setting the rate of evaporation. The influence of the external mass fraction Ye is to adjust the surface concentration and temperature slightly, but does not strongly affect the evaporation rate. As a result, the evaporation process is one of heat transfer control.

Evaluating Surface Conditions--Convecting Environments

For the present study involving a convecting flow field, the balance of heat and mass fluxes are performed using the Sh and Nu correlations and local external driving potentials. Contrary to the

quiescent analysis described above, this study does not assume the Lewis number to be 1, but includes relations for the mass and thermal diffusivities. The values for all properties and surface potentials are periodically updated based on a change in the local Reynolds number. These property relations were taken from various sources and are given in the appendix.

Effect of Pressure Oscillations

In determining the mole fraction of the evaporating liquid in the gas at the surface, the local environmental pressure needs to be specified. The maximum oscillation pressure in the pulse combustor occurs in the combustion chamber and is approximately ±10 kPa (±10% change). Since the oscillation pressure in the tailpipe is less than that in the combustion chamber (varying as a 1/4 sinusoid from the combustion chamber to the end of the tailpipe), it is assumed that the pressure remains constant at the mean value of one atmosphere. Neglecting the pressure oscillation ignores the associated surface temperature changes which are about 6 to 8 K. However, the change in the heat transfer driving potential will be small and, since the process is heat transfer controlled, so will be the evaporation rate. For small changes in the pressure, p', the temperature at the surface can be shown to change as $Ts' = T_o^2 Rp'/P_o h_{fg}$, where Ts' is the fluctuating surface temperature due to fluctuating pressure p', T_o is the average surface temperature of the liquid whose gas phase species is at the average partial pressure P_o, R is the gas constant, and h_{fg} is the heat of vaporization. Finally, neglecting the pressure oscillations also neglects the changes in the transport diffusivities which are inversely proportional to the pressure. However, since the boundary layers for mass, momentum and energy are, to first order, proportional to the square root of the diffusivities, the effect of the ±10% pressure oscillations are reduced to only ±5% for the boundary layer. Therefore the changes in the transports of mass, momentum and energy are small (the pressure has a weak affect on the transport coefficients μ, k, and ρD).

Tailpipe Gas Model

A brief description of the gas phase motion in a typical pulse combustor will be given. For a more detailed description of pulse combustors see Keller et al. (1989). Temperature and velocity profiles (axial and transverse) in the tailpipe of a "Helmholtz" type pulse combustor have been determined experimentally by Dec and Keller (1988) and Dec et al. (1988), and numerically by Barr et al. (1988). Figure 2 shows experimental data on the cycle resolved tailpipe gas temperature and velocity as well as combustion chamber pressure for a typical pulse combustion operating condition, Dec and Keller (1988). Figure 2 shows that both the velocity and pressure are sinusoidal. The temperature has a peak-to-peak fluctuation of approximately 200 K through the cycle. Although this may appear to be large, the change is small relative to the total driving potential (<15%). Moreover, for the droplets studied here, the droplet lifetimes are longer than several cycles providing an averaging effect for these fluctuations. Should detailed information on the droplet evolution be required, these fluctuations should probably be considered. From this data as well as data on the axial profiles of mean temperature and velocity oscillation amplitude, it is found that the gas temperature can be effectively modeled as a linearly decreasing function of axial location starting at the inlet to the tailpipe, while the velocity amplitude in the tailpipe can be modeled as a linearly increasing function of location. It is assumed that the temperature decreases in value based on experimentally determined input parameters defining the inlet and exit temperatures as well as the tailpipe length. The oscillating velocity component was described by a relation based on an input of the exit velocity amplitude with the inlet velocity being 80% of that at the exit, Dec and Keller (1988). The mean velocity component in the tailpipe was also specified based on experimental values, Dec and Keller (1988). Finally, it is assumed that the gas composition was that of stoichiometric methane-air combustion products.

Calculations for the droplet histories were made for the different pulse combustion operating cases listed in Table 1. The nominal values for an experimental pulse combustor are in bold. The parameters in the table are defined in the nomenclature.

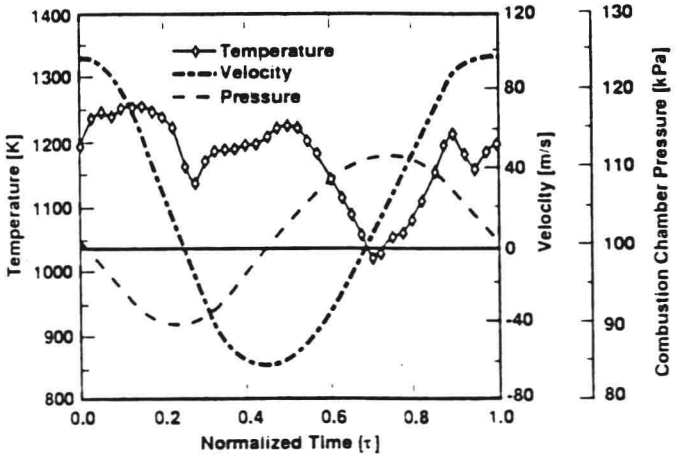

Figure 2. Pulse Combustor Tailpipe Profiles of Velocity and Temperature, from Dec et al. (1988). The velocity and pressure are very sinusoidal and the temperature fluctuations are small relative to the absolute temperature.

TABLE 1 Pulse Combustor Conditions

Case	Uo	Um	Te_i	Te_e	ω	Le
1	50	15	1500	700	100	0.88
2	75	15	1500	700	100	0.88
3	100	15	1500	700	100	0.88
4	75	15	1500	700	80	0.88
5	75	15	1500	700	120	0.88
6	75	15	1300	500	100	0.88
7	75	15	1700	800	100	0.88
	75	**15**	**1500**	**700**	**83**	**0.88**
8	-	15	1500	700	0	0.88
Units:	m/s	m/s	K	K	Hz	m

For all cases, the initial droplet size and velocity was 100 μm and 2 m/s.

RESULTS

Since the history of a droplet size in a quiescent environment follows the D^2 Law which can be written in terms of the droplet radius as:

$$R^2 = R_0^2 - \beta t \qquad (20)$$

where β is the evaporation coefficient, the results for the droplet size are presented as R^2 vs. time.

Figure 3 shows the droplet size vs. time for cases 1,2,3,8. As expected, the evaporation rate increases with pulsation amplitude. For the same four cases, the droplet position vs. time is presented in Figure 4. For all cases the droplet has evaporated before exiting the 880 mm tailpipe (the position where a droplet is entirely evaporated is denoted by an 'x').